Histochem Cell Biol
DOI 10.1007/s00418-011-0862-7

ORIGINAL PAPER

The effect of inflammation on the expression and distribution of the MAS-related gene receptors MrgE and MrgF in the murine ileum

Leela R. Avula · Roeland Buckinx · Katrien Alpaerts · Anna Costagliola · Dirk Adriaensen · Luc Van Nassauw · Jean-Pierre Timmermans

Accepted: 29 August 2011

Abstract The MAS-related gene (Mrg) receptor MrgE has been suggested to be expressed at all tissue levels involved in pain sensation and to influence the expression of another Mrg receptor, MrgF. Given the knowledge on the role of the enteric nervous system (ENS) in sensation, and the plasticity of enteric neurons during intestinal inflammation, it can be hypothesized that MrgE is expressed in enteric neurons, and that MrgE and MrgF change expression in intestinal inflammatory conditions. Therefore, we aimed to reveal the expression details of MrgE and MrgF in the murine ileum in normal and inflamed conditions. Using reverse transcriptase-PCR, quantitative-PCR and immunohistochemistry, we compared the ileum of non-inflamed control mice with that of two models of intestinal inflammation, i.e. intestinal schistosomiasis and chemically induced ileitis. MrgE and MrgF mRNAs were detected in control and inflamed conditions. MrgE and MrgF mRNAs showed a trend towards downregulation during intestinal schistosomiasis and a significant reduction during ileitis. MrgE and MrgF receptors were expressed in distinct enteric neuronal subpopulations, such as the sensory, secretomotor and vasodilator neurons, and in nerve fibres in the tunica muscularis and lamina propria of control and inflamed ileum. Only a minor proportion of enteric neurons co-expressed MrgE and MrgF. The number of enteric neurons expressing MrgE and MrgF receptors was significantly reduced during intestinal schistosomiasis and ileitis. This is the first report on the expression of MrgE and MrgF in the ENS in (patho)physiological conditions. The expression of MrgE and MrgF in enteric neurons was negatively affected by inflammation.

Keywords MAS-related gene · Enteric neurons · Intestinal inflammation · MrgE · MrgF · Ileum

L. R. Avula · R. Buckinx · K. Alpaerts · D. Adriaensen · L. Van Nassauw · J.-P. Timmermans (✉)
Laboratory of Cell Biology and Histology,
Department of Veterinary Sciences, University of Antwerp,
Groenenborgerlaan 171, 2020 Antwerp, Belgium
e-mail: jean-pierre.timmermans@ua.ac.be

A. Costagliola
Department of Biological Structures, Functions and Technology,
University of Naples "Federico II", Via F. Delpino 1,
80137 Naples, Italy

L. Van Nassauw
Laboratory of Human Anatomy and Embryology,
Faculty of Medicine, University of Antwerp,
Groenenborgerlaan 171, 2020 Antwerp, Belgium

Introduction

A family of orphan G protein-coupled receptors (GPCRs), also designated as MAS-related gene (Mrg) receptors or sensory neuron-specific GPCRs, has been identified in rodents and humans (Dong et al. 2001; Lembo et al. 2002; Young et al. 1986) consisting of members that are predominantly expressed in sensory neurons of dorsal root ganglia (DRG) and trigeminal ganglia (TG) (Breit et al. 2006; Burstein et al. 2006; Dong et al. 2001; Gustafson et al. 2005; Hager et al. 2008; Lembo et al. 2002; Liu et al. 2008; Rau et al. 2009; Wang and Zylka 2009; Zhang et al. 2005; Zylka et al. 2003), and implicated in nociception (Chang et al. 2009; Chen and Ikeda 2004; Cox et al. 2008; Crozier et al. 2007; Grazzini et al. 2004; Rau et al. 2009). Mrg receptors originate mainly from four different MAS-related G protein-coupled receptor member genes, i.e. *MrgX* in humans and rhesus monkeys, and *MrgA*, *MrgB* and *MrgC* in rodents. The *MrgX* genes have no direct orthologues in

Published online: 13 September 2011

rodents, but appear to be closely related to the MrgA receptors. In rodents, the Mrg family also contains six single-copy genes, known as *MrgD*, *MrgE*, *MrgF*, *MrgG*, *MrgH* (*GPR90*) and *MAS1*, which have clear human orthologues (Burstein et al. 2006; Dong et al. 2001; Lembo et al. 2002; Zhang et al. 2005; Zylka et al. 2003). In mice due to the species-specific atypical expansion, the Mrg family consists mainly of three large MrgA, MrgB and MrgC subfamilies, which together with the products of the single-copy genes comprise ~50 distinct members (Zylka et al. 2003).

While Mrg receptors are still classified as orphan receptors, some have recently been de-orphaned by the identification of ligands activating their cognate receptors. RF-amide neuropeptides distinctively activate the mouse MrgA1, MrgA4, MrgC11 and MAS1 receptors (Dong et al. 2001; Han et al. 2002) and rat MrgC (Grazzini et al. 2004). Adenine is an endogenous ligand for MrgA (Bender et al. 2002) and β-alanine a ligand for MrgD (Shinohara et al. 2004), while MrgD is also able to respond to ATP (Dussor et al. 2008). Angiotensin metabolites are capable of stimulating MrgD and MrgG (Gembardt et al. 2008), while salusin β is a surrogate ligand for MrgA1 (Wang et al. 2006). Human and rhesus monkey MrgX2 is activated by proadrenomedullin N-terminal peptides and cortistatin (Burstein et al. 2006; Kamohara et al. 2005; Robas et al. 2003). Basic secretagogues have been suggested to activate G proteins through MrgX2 on human mast cells, indicating a role in inflammatory responses (Tatemoto et al. 2006). Another study revealed that mast cells can secrete an RF-amide neuropeptide that stimulates Mrg receptors present on primary afferent nerves (Lee et al. 2008). Bovine adrenal medulla peptide 22 activates human MrgX1 and rat MrgC (Breit et al. 2006; Grazzini et al. 2004; Lembo et al. 2002). Pyridazinones are small-molecule agonists for human MrgX1 (Wroblowski et al. 2009). At present, only putative antagonists, i.e. 2,3-disubstituted azabicyclo-octanes, have been described for the human MrgX1 receptor (Kunapuli et al. 2006).

Apart from the selective expression of some Mrg receptors in nociceptive neurons of DRG and TG, only scarce information is available on the expression and distribution patterns of the Mrg members in other tissues and organs. Human MrgX2 mRNA has also been detected in the brain, pituitary gland, thyroid gland, gastrointestinal (GI) tract, lungs and gonads, while immunolocalization was found to be limited to the neurohypophysis, testis, vascular endothelial cells, scattered lymphocytes and enteric ganglia (Allia et al. 2005; Robas et al. 2003). It has been demonstrated that mouse MrgC11 is also expressed in nodose ganglia (Lee et al. 2008), and mRNAs for MrgA and MrgC have also been observed in rat brain and several non-neuronal tissues, including the GI tract (Gustafson et al. 2005). Apart from being present in DRG in rat, MrgD mRNA has also been detected in the testis, whereas MrgE mRNA has been detected in brain, spinal cord and sciatic nerve (Milasta et al. 2006). mRNA of rat MrgF has been detected in gut, uterus, vas deferens, brain and aorta (Ross et al. 1990). In mouse, macaque and human, MrgE has been found to be expressed in brain and spinal cord (Cox et al. 2008; Zhang et al. 2005), as also observed for mouse MrgF and MrgH (Cox et al. 2008).

It has been suggested that MrgE is expressed at all tissue levels involved in pain sensation (Cox et al. 2008). Moreover, MrgE has been suggested to modulate the function of other Mrg receptors due to heteromerization (Milasta et al. 2006), or to influence their expression levels, as seen for MrgF (Cox et al. 2008). These data led us to speculate that MrgE and MrgF are expressed in the enteric nervous system (ENS), since enteric neurons are known to be a source of sensory innervation in the GI tract enabling the decentralized gut to perform complex reflex functions (Blackshaw et al. 2007). Further, changes in MrgE and MrgF expression can be expected in intestinal inflammatory conditions as a consequence of the plasticity of the ENS and the sensitization of sensory pathways during intestinal inflammation (Bielefeldt et al. 2009; Giaroni et al. 1999; Lomax et al. 2005; Mawe et al. 2009; Vasina et al. 2006), and such changes may vary depending on the nature of the inflammatory stimulus. However, to date, no detailed expression data on MrgE and MrgF are available in the gut in normal or inflamed circumstances. All the above reasons initiated us to compare the ileum of healthy non-inflamed control mice with that of two murine models of intestinal inflammation, i.e. (1) *Schistosoma mansoni*-induced intestinal schistosomiasis and (2) trinitrobenzene sulphonic acid (TNBS)-induced ileitis. Intestinal schistosomiasis is a parasitic helminth disease, which at the acute stage involves a granulomatous immunopathology with a Th2-type inflammatory response directed against parasite eggs that lodge in the liver and intestine (Vella and Pearce 1992; Yolles et al. 1949). TNBS-induced ileitis at the acute stage is characterized by acute mucosal damage and a localized Th1/Th17-type inflammatory reaction in response to the haptenating agent (Elson et al. 1996; Pontell et al. 2009; Ruyssers et al. 2009). Our study, using PCR and immunohistochemistry techniques, enabled us to disclose the effect of inflammation on the expression and distribution of MrgE and MrgF in the murine ileum.

Materials and methods

Animals

Studies were performed on adult male C57BL/6J mice (Janvier, Le Genest St Isle, France) provided with standard

pellet diet and water ad libitum, and housed in a 12-/12-h light/dark cycle at constant temperature (22°C). Animals were divided into three experimental groups: healthy control animals, mice infected with *S. mansoni* and mice in which ileitis had been induced with TNBS ($n = 6$ in each group). All experimental procedures were approved by the ethical committee of the University of Antwerp. The animals in the three experimental groups were age matched at the time of tissue retrieval.

To prepare the *S. mansoni*-infected group, mice were infected with *S. mansoni* according to the method of Yolles et al. (1949). Briefly, the mice were anesthetized with an intraperitoneal injection of sodium pentobarbital (60 mg kg^{-1}; Nembutal; Sanofi, Brussels, Belgium), and 1 ml of sterile water containing 130 freshly shed cercariae of a Puerto Rico strain of *S. mansoni* was intraperitoneally injected. The mice were then killed 8 weeks post-infection at the acute stage of intestinal schistosomiasis. The cycle of *S. mansoni* was maintained by passage through *Biomphalaria glabrata* snails.

In the TNBS-induced ileitis group, ileitis was induced by laparotomy according to a modified procedure of Pontell et al. (2009). Briefly, after fasting for 24 h, mice were anesthetized using a mix of medetomidine (0.5 mg kg^{-1}; Domitor; Pfizer, New York, NY, USA) and ketamine (50 mg kg^{-1}; Anesketin; Eurovet, Bladel, The Netherlands) dissolved in a physiological solution and administered intraperitoneally (Yolles et al. 1949). After having been shaved and disinfected, the lower abdomen was incised and the ileum was exteriorized. A volume of 0.1 ml TNBS (25 mg ml^{-1} in 25% ethanol; Sigma-Aldrich, St. Louis, MO, USA) was injected into the lumen of the ileum 2 cm proximal to the ileo-caecal junction. Before closing the midline incision, a solution containing marbofloxacin (2 mg kg^{-1}; Marbocyl; Vetoquino S.A., Lure Cedex, France) was injected into the peritoneal cavity. Following surgery, the animals were maintained in a controlled environment for 24 h and subsequently killed.

Tissues

All animals were killed by cervical dislocation followed by exsanguination. The ileum of each animal was removed and washed in Krebs solution (117 mM NaCl, 5 mM KCl, 2.5 mM $CaCl_2 \cdot 2H_2O$, 1.2 mM $MgSO_4 \cdot 7H_2O$, 25 mM $NaHCO_3$, 1.2 mM $NaH_2PO_4 \cdot 2H_2O$ and 10 mM glucose; pH 7.4). Three 5 mm parts were removed at the distal end of each ileum. One of these parts was fixed for 2 h at room temperature in 4% paraformaldehyde in 0.1 M phosphate buffer (PF; pH 7.0), processed for paraffin embedding and 5 µm-thick sections were stained with haematoxylin and eosin (HE). Another part was snap-frozen in liquid nitrogen and stored at −80°C for RNA isolation. The third part was fixed for 2 h at room temperature in Zamboni's fixative (PF containing 10% picric acid), washed in 0.01 M phosphate-buffered saline (PBS; pH 7.4) and rinsed according to the procedure of Llewellyn-Smith et al. (1985). Subsequently, they were incubated overnight in PBS containing 20% sucrose at 4°C, embedded in OCT-embedding medium (Pelko Int., Torrance, CA, USA), cryostat-sectioned at 12 µm and thaw-mounted on poly-L-lysine-coated slides. The remaining part of the ileum was opened along the mesenteric border and pinned out in a Sylgard-lined Petri dish. Because of the faint staining within the neuronal somata for the receptors and some neuropeptides used in this study, to enhance the immunoreactivity (IR), this part of the ileum was, prior to fixation, maintained in organotypic culture, in a medium containing colchicine as previously described (Van Nassauw et al. 2002). Fixation and clearing for this part of the ileum occurred as described for the tissue parts processed for cryosectioning. Whole mounts containing the myenteric and submucous plexus were then prepared by dissecting the external musculature and submucosa/mucosa apart and removing the circular muscle layer and mucosa, respectively.

RNA treatment

Total RNA isolation and processing were performed as previously described (Van Op den bosch et al. 2007). Briefly, total RNA was isolated from ileal segments using Trizol reagent (Life Technologies Inc., Gaithersburg, MD, USA). Further, a purification treatment was performed on 5 µg of RNA using the Turbo DNA-free™ kit (Ambion, Austin, TX, USA). A total amount of 1 µg DNase-treated RNA was reverse transcribed using the Transcriptor First Strand cDNA synthesis kit (Roche, Mannheim, Germany). The efficiency of reverse transcription was verified using control RNA and primers included in this kit.

Reverse transcriptase (RT)-PCR

The primers for the mRNAs of MrgE, MrgF and the internal controls, glyceraldehyde 3-phosphate dehydrogenase (GAPDH) and hypoxanthine phosphoribosyltransferase (HPRT), were designed using the Lightcycler Probe Design 2 software (Roche) and listed in Table 1. RT-PCR was performed on an MJ Mini Cycler (Biorad, Hercules, CA, USA), and cDNA of DRG of healthy control mice was used as a positive control, while DNase-treated RNA samples served as negative controls. PCR products were prepared in a total reaction volume of 25 µl, containing 12.5 µl of HotstarTaq Master Mix (Qiagen, Hilden, Germany), 0.25 µl (0.4 µM) each of forward and reverse primers and 1 µl cDNA that was diluted 1:5. After denaturation at 95°C for 15 min, 40 amplification cycles were performed consisting

Table 1 5′→3′ primer sequences used for RT-PCR and q-PCR

Annealing temperatures (T^A) of the primers and the temperature at which the fluorescence signal was measured (T^M) for q-PCR

FP forward primer, *RP* reverse primer

Gene	Primer	Sequence 5′→3′	T^A (°C)	T^M (°C)
GAPDH	GAPDH FP	TGGCAAAGTGGAGATTGTTGCC	64	83
	GAPDH RP	AAGATGGTGATGGGCTTCCCG		
HPRT	HPRT FP	CCTAAGATGAGCGCAAGTTGAA	60	84
	HPRT RP	CACAGGACTAGAACACCTGCTAA		
MrgE	MrgE FP	CCTTCCTTTAGTGAGGGATAAATGA	57	83
	MrgE RP	TTGCCTTCTGGCAGTGAT		
MrgF	MrgF FP	CCGGAAACTGTTCATGGG	57	84
	MrgF RP	AGCAGCAGGAAGATATAGTTTG		

of a denaturation phase at 94°C for 1 min, an amplification phase at 54–60°C for 30 s and an elongation phase at 72°C for 90 s, followed by a final extension step at 72°C for 10 min. Using 2% agarose gel, the amplification products were separated and visualized under UV illumination.

Quantitative (q)-PCR

The same primers as mentioned above for RT-PCR were used for q-PCR. All q-PCR experiments were performed using the Lightcycler FastStart DNA Master PLUS SYBR Green I kit (Roche) in a reaction volume of 20 µl, containing 3 mM $MgCl_2$, 0.5 µM of each forward and reverse primer, 2 µl SYBR Green Master Mix and 2 µl cDNA suspension. After denaturation, 55 amplification cycles were performed, consisting of a denaturation step at 95°C for 15 s, a primer-specific annealing temperature for 10 s and amplification at 72°C for 15 s. Melting curve analysis and agarose gel electrophoresis were performed at the end of each reaction to ensure the specificity of the amplification products and the absence of artefacts. All reactions were performed in triplicate. The MrgE and MrgF mRNA levels in all experimental groups were quantified by q-PCR normalized to the combined mRNA levels of GAPDH and HPRT and statistically analysed using a Student's *t* test. Results are expressed as mean values ± standard error of means. Significance was assumed at $P < 0.05$.

Immunohistochemistry

All immunohistochemical incubations were carried out at room temperature. Unless indicated otherwise, washes with PBS were performed between incubations. The antibodies used in this study, as well as their respective dilutions, are listed in Table 2. To block non-specific immunoglobulin interactions and to enhance permeability, cryosections and whole mounts were immersed in 0.1 M PBS (pH 7.4) with 0.05% thimerosal (PBS*), containing 10% normal horse serum (NHS) and 1% Triton X-100 for 1 h. Next, they were incubated for 16 h with a mixture of primary antibodies raised in different species and diluted in PBS* containing 10% NHS and 0.1% Triton X-100. Subsequently, after being rinsed in PBS, the tissues were incubated for 1 h with the appropriate secondary antibodies diluted in PBS* containing 1% NHS to visualize immunostaining. The cryosections and whole mounts were evaluated with fluorescence and confocal microscopy.

Using two primary antisera that were raised in the same species to detect putative co-expression of MrgE and MrgF, a sequential immunostaining technique was performed according to the method of Negoescu et al. (1994). In this procedure, a biotinylated polyclonal monovalent Fab fragment and fluorochrome-conjugated streptavidin were used to visualize the first primary antibody. After detection of the first antigen, the samples were washed prior to incubation for 2–4 h with unlabelled Fab fragments diluted in PBS, directed against the first primary antibody to block residual binding sites on the first primary antibodies (Lewis Carl et al. 1993). Next, they were rinsed in PBS and the second antigen was detected and visualized using a standard fluorophore-labelled secondary antibody.

Negative controls were those in which the primary antibodies were omitted. The specificity of secondary antisera was tested by omitting the primary antisera separately on interference controls. Because the appropriate immunogens were not commercially available, antibody specificity for the antibodies directed against MrgE and MrgF was verified by immunoblotting and immunoenzymatic staining of paraffin-embedded brain sections of control mice, in which the distribution of MrgE and MrgF was previously described (Chang et al. 2009; Zhang et al. 2005). Furthermore, to reveal putative cross-reactivity with other proteins including the other Mrg receptors, the specificity of the immunogen sequences was verified by using the BLAST program (http://blast.ncbi.nlm.nih.gov/Blast.cgi).

Histological evaluation

Histological evaluation of the HE-stained paraffin sections was performed by light microscopy by two independent observers blinded to the disease status of the animals.

Table 2 List of antibodies used for immunohistochemistry

Antigen	Host	Dilution	Source
Primary antibodies			
Mas-related gene E	Rabbit	1:2,000	Abcam, Cambridge, UK (ab65432)
Mas-related gene F	Rabbit	1:1,500	Abcam (ab65546)
Protein gene product 9.5	Guinea pig	1:500	GeneTex Inc., San Antonio, CA, USA (GTX10410)
Protein gene product 9.5	Guinea pig	1:500	Chemicon, Poole, UK (AB5898)
Calcitonin gene-related peptide	Goat	1:2,500	Abcam, Cambridge, UK (ab36001)
Calretinin	Goat	1:12,000	Swant, Switzerland (CG1)
Calbindin	Goat	1:200	Santa Cruz Biotechnology, Santa Cruz, CA, USA (sc-7691)
Neuronal nitric oxide synthase	Goat	1:1,000	Abcam (ab1376)
Vasoactive intestinal peptide	Goat	1:100	Santa Cruz Biotechnology (sc-7841)
Substance P	Guinea pig	1:1,000	Abcam (ab10353)
Mouse mast cell protease-1	Sheep	1:2,000	Moredun Scientific, Edinburgh, UK (MS-RM8)

Antigen	Dilution	Source
Secondary antibodies		
FITC-conjugated donkey anti-guinea pig IgG	1:150	Jackson ImmunoResearch Laboratories, West Grove, PA, USA
FITC-conjugated donkey anti-goat IgG	1:200	Jackson ImmunoResearch Laboratories
Cy3-conjugated donkey anti-rabbit IgG	1:400	Jackson ImmunoResearch Laboratories
FITC-conjugated donkey anti-sheep IgG	1:200	Jackson ImmunoResearch Laboratories
Biotinylated Fab fragments of goat anti-rabbit IgG	1:2,000	Rockland, Gilbertsville, PA
FITC-conjugated streptavidin	1:1,000	Jackson ImmunoResearch Laboratories
Unlabelled Fab fragments of goat anti-rabbit IgG	1:100	Jackson ImmunoResearch Laboratories

Cy3 cyanine 3, *FITC* fluorescein isothiocyanate

Quantitative analysis

Quantitative analysis of the immunostainings was performed as previously described (Van Nassauw et al. 2002). The immunoreactive nerve cell bodies in the myenteric and submucous ganglia were counted per visual field (0.3 mm^2) in whole-mount preparations. Ten randomly chosen fields in each whole mount were analysed. The percentage of neurons expressing MrgE, MrgF, or one of the neurochemical markers—calretinin (CRT), calbindin (CB), neuronal nitric oxide synthase (nNOS), substance P (SP) and vasoactive intestinal peptide (VIP)—was calculated using protein gene product 9.5 (PGP) as a pan-neuronal marker. Furthermore, co-expression of MrgE or MrgF with other neuronal markers, such as CRT, CB, nNOS and SP, in the myenteric ganglia was also quantitatively analysed. The same methods were applied to calculate the co-expression values of MrgE or MrgF with CRT and VIP in the submucous ganglia. In addition, the co-expression of MrgE and MrgF in myenteric and submucous ganglia was also quantified. Two whole mounts per animal and six animals per experimental group were analysed for each double immunolabelling experiment. Statistical analyses were performed by Student's *t* test and Mann–Whitney test. Results are expressed as mean values ± standard error of means. Significance was assumed at $P < 0.05$.

Results

Histology

No pathological signs of inflammatory activity were observed in the ileum of the control animals (Fig. 1a). The ileum of *S. mansoni*-infected mice was characterized by the presence of granulomas surrounding the entrapped parasite eggs in the submucosa and mucosa, thickening of the tunica muscularis and broadening of the intestinal villi as previously described (Fig. 1b). The inflammatory response consisted of a diffuse mucosal inflammation and a granulomatous reaction as previously described (Bogers et al. 2000). Observations made in TNBS-induced ileitis were similar to those described in guinea pig (Pontell et al. 2009). The villi showed indications of necrosis, resulting in debris in the lumen, and were ablated, although signs of restoration of the mucosal epithelium were observed. Subepithelial cysts and a high number of immune cells within the lamina propria or closely associated with the enteric ganglia were also seen (Fig. 1c).

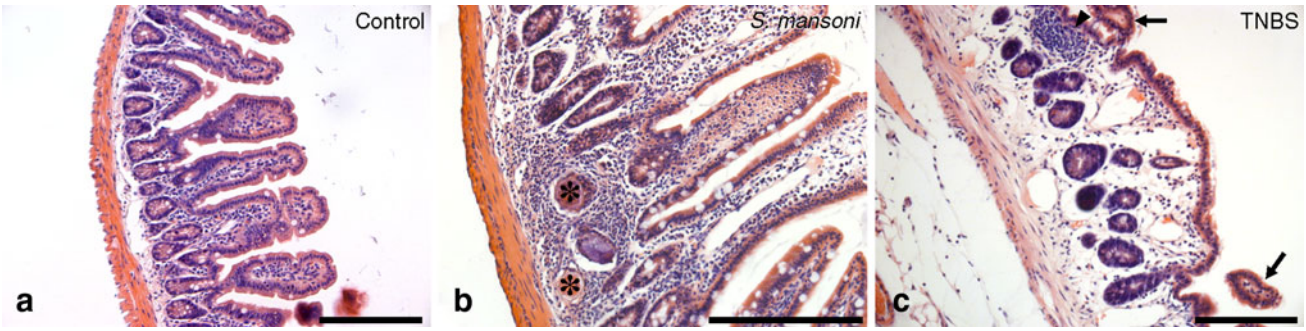

Fig. 1 Histological evaluation of the HE-stained paraffin sections of control and inflamed ileum. **a** No pathological signs of inflammatory activity were observed in the control ileum. **b** The *S. mansoni*-infected ileum was characterized by the presence of granulomas with entrapped parasite eggs (*asterisk*), broadening of the villi and thickening of the tunica muscularis. **c** The TNBS-treated ileum showed ablated and broken villi, signs of restoration of the mucosal epithelium (*arrows*), subepithelial cysts and a high number of immune cells in the lamina propria (*arrowhead*) and in the vicinity of enteric ganglia. *Scale bar* 200 µm. *Control* control ileum, *S. mansoni S. mansoni*-infected ileum, *TNBS* TNBS-treated ileum

RT-PCR and q-PCR

The non-reverse-transcribed RNA samples did not yield any amplification products, thus excluding contamination with genomic DNA. RT-PCR detected the expression of MrgE and MrgF mRNAs in all tissue samples of control, *S. mansoni*-infected or TNBS-treated ileum (Fig. 2a, b, respectively). Quantification of the MrgE and MrgF mRNA levels revealed that the mRNA levels for both these Mrg members were virtually similar in the ileum of control animals. In comparison with the control ileum, MrgE and MrgF mRNA levels showed a non-significant trend towards downregulation (MrgE: $P = 0.096$; MrgF: $P = 0.095$) in the *S. mansoni*-infected ileum, while both MrgE and MrgF mRNA levels were significantly decreased (MrgE: $P = 0.028$; MrgF: $P = 0.010$) in the TNBS-treated ileum (Fig. 2c, d).

Immunohistochemistry

Omission of the primary antibodies did not yield any immunofluorescent signal. Interference control stainings did not show any cross-reactivity of the secondary antibodies. Immunoblotting detected MrgE and MrgF at their predicted band sizes, i.e. at 35 and 38 kDa, respectively. Immunostaining of the brain sections revealed MrgE and MrgF IR in neurons as previously described (Chang et al. 2009; Zhang et al. 2005) (data not shown). The immunogens used for the development of MrgE and MrgF antibodies were synthetic peptides corresponding to an internal part of mouse MrgE (aa 100–200) and of mouse MrgF (aa 130–230), respectively. The BLAST search showed that the most potent topological domains within these regions for MrgE and MrgF displayed no significant cross-reactivity or homology with other proteins, indicating that the antibodies directed against MrgE and MrgF will specifically bind to their respective proteins. The above observations thus confirm the specificity of the antibodies used in our study.

Cryosections of the control ileum showed MrgE and MrgF IR in neuronal somata and nerve fibres in both enteric plexuses and in nerve fibres in the tunica muscularis and in the lamina propria (Fig. 3a, b). A similar distribution for both Mrg receptors was observed in cryosections of the *S. mansoni*-infected ileum (Fig. 3c, d). The acute phase of intestinal schistosomiasis, i.e. at 8 weeks post-infection, is characterized by a significant recruitment of mucosal mast cells in the mucosa and submucosa. Double immunostaining including an antibody directed against the enzyme mouse mast cell protease-1, which is exclusively expressed in mucosal mast cells (De Jonge et al. 2002), did not show expression of MrgE or MrgF in mucosal mast cells (data not shown). However, an increased number of MrgE- and MrgF-positive nerve fibres were observed in the lamina propria of the villi (Fig. 3c, d), in line with the observed sprouting of nerve fibres in the lamina propria in intestinal schistosomiasis (De Jonge et al. 2003; Van Op den bosch et al. 2007). Double immunostaining using an antibody directed against calcitonin gene-related peptide (CGRP), a valid marker for extrinsic primary afferent neurons (EPANs) in the murine ileum (De Jonge et al. 2003), demonstrated that the MrgE- and MrgF-positive nerve fibres in the lamina propria of the villi extensively co-expressed CGRP (Fig. 3e, f). The distribution for both Mrg receptors in the TNBS-treated ileum was similar to that observed in the control ileum. However, the IR observed in neuronal perikarya in the enteric plexuses, nerve fibres in the tunica muscularis and the lamina propria was not prominent, especially not in the villi, most of which were ablated (Fig. 3g, h).

In whole mounts, MrgE and MrgF IR were expressed in neuronal somata and nerve fibres. The results of the quantitative analysis of the whole mounts are shown in Table 3.

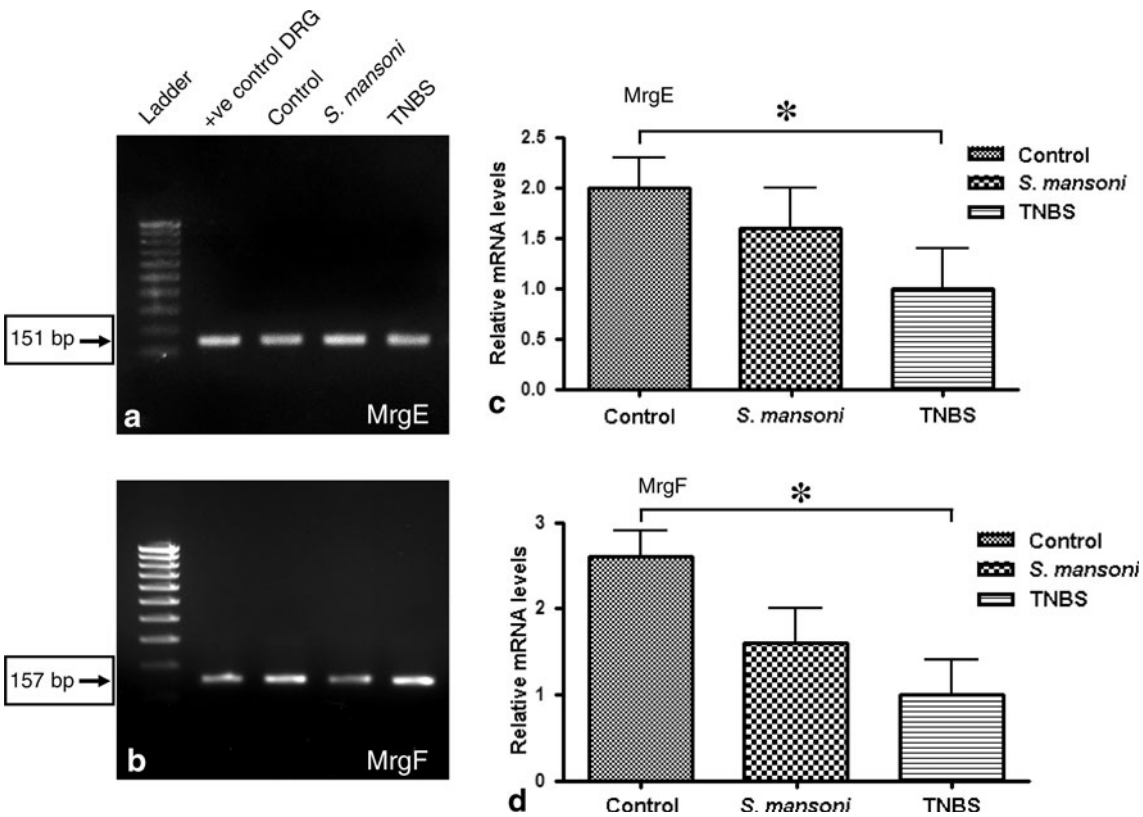

Fig. 2 RT-PCR and q-PCR for MrgE and MrgF in control and inflamed ileum. RT-PCR detection of MrgE (**a**) and MrgF (**b**). *Lane 1* DNA ladder, *lane 2* DRG cDNA from control animals as a positive control, *lane 3* cDNA of the control ileum, *lane 4 S. mansoni*-infected ileal cDNA, *lane 5* cDNA of the TNBS-treated ileum. *bp* base pairs. MrgE and MrgF cDNAs were detected in control, *S. mansoni*-infected and TNBS-treated conditions. Quantification of the MrgE (**c**) and MrgF (**d**) mRNA levels in the control and inflamed ileum relative to the normalized GAPDH/HPRT mRNA level. Compared to the control ileum, MrgE and MrgF mRNA levels showed a trend towards downregulation, which was not significant in the *S. mansoni*-infected ileum, while in the TNBS-treated ileum these mRNA levels showed a significant decrease (*$P < 0.05$). *Control* control ileum, *S. mansoni S. mansoni*-infected ileum, *TNBS* TNBS-treated ileum

In the ENS of the control ileum, 17 ± 2% of the PGP-immunoreactive (ir) myenteric neurons (Fig. 4a) and 16 ± 3% of the PGP-ir submucosal neurons (Fig. 4b) expressed MrgE IR. The chemical coding of the MrgE-ir myenteric neurons revealed that 18 ± 2% of these neurons co-expressed CRT (Fig. 4c, d), 50 ± 3% displayed CB IR (Fig. 4e), 16 ± 3% yielded nNOS IR (Fig. 4f, g) and only 6 ± 3% exhibited SP IR (Fig. 4h). In the submucous plexus, 80 ± 3% of the MrgE-ir neurons expressed CRT IR (Fig. 4i, j) and 58 ± 3% displayed VIP IR.

In the *S. mansoni*-infected ileum, the proportion of PGP-ir enteric neurons expressing MrgE IR showed a non-significant decrease in the myenteric plexus (11 ± 3%) and was significantly lower in the submucous plexus (8 ± 3%). This significant reduction in MrgE IR was found in CRT-expressing, VIP-negative submucosal neurons (Table 3), especially in the vicinity of the entrapped parasite eggs (Fig. 4k, l). The proportional distribution of MrgE in myenteric neurons was not significantly changed in this condition.

In the TNBS-treated ileum, a significant reduction in the proportional expression of PGP-ir myenteric neurons expressing MrgE IR (5 ± 2%) was observed (Fig. 4m, n), although the percentage of PGP-ir submucosal neurons expressing MrgE IR was non-significantly reduced (10 ± 4%). In the myenteric plexus, a higher proportional expression of CB (86 ± 3%) was detected in the MrgE-ir neurons, but overall there was a significant reduction in MrgE IR in CB-expressing neurons (Table 3). The percentage of MrgE-ir neurons exhibiting nNOS IR (5 ± 2%) (Fig. 4o, p) and the percentage of nNOS-ir neurons exhibiting MrgE were reduced (Table 3). The submucosal neurons did not show any significant changes in the proportional distribution of MrgE.

In the control ileum, MrgF IR was found in 12 ± 2% of the PGP-ir myenteric neurons (Fig. 5a) and in 9 ± 2% of the PGP-ir submucosal neurons (Fig. 5b). Double labelling showed that 12 ± 2% of these myenteric neurons co-expressed CRT (Fig. 5c, d), while 68 ± 3% co-expressed CB (Fig. 5e, f), 15 ± 2% nNOS and 25 ± 3%

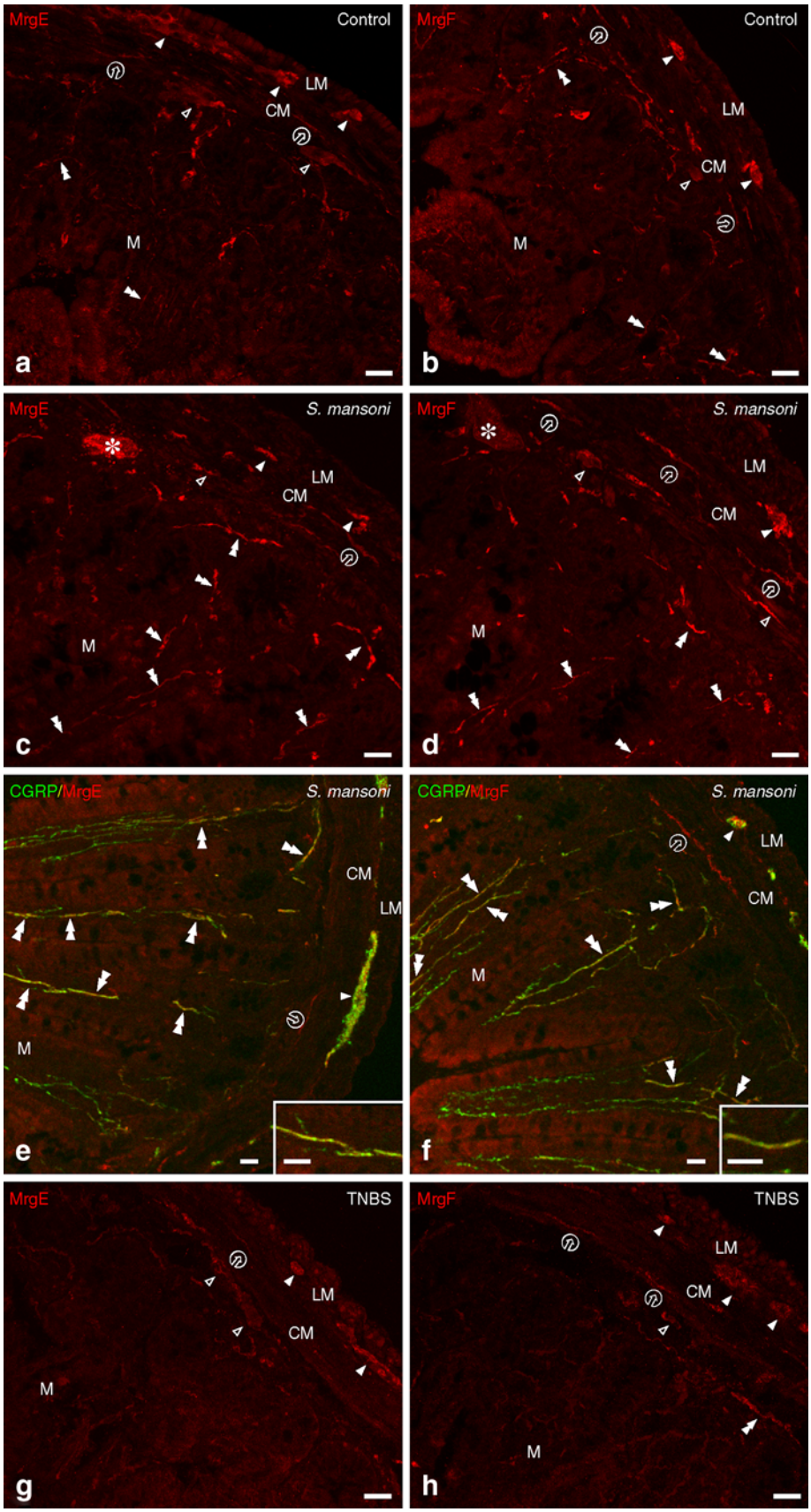

Fig. 3 Immunohistochemical detection of MrgE and MrgF on cryosections. In the control (**a**, **b**), *S. mansoni*-infected (**c**–**f**) and the TNBS-treated (**g**, **h**) ileum, expression of MrgE (**a**, **c**, **e**, **g**) and MrgF (**b**, **d**, **f**, **h**) was detected in myenteric neurons (*arrowheads*), submucosal neurons (*open arrowheads*), in nerve fibres in the tunica muscularis (*encircled open arrow*) and the lamina propria of the villi (*double arrowheads*). Compared to the control ileum, the number of MrgE- and MrgF-ir neuronal perikarya in the enteric plexuses was lower in the *S. mansoni*-infected ileum, whereas the numbers of MrgE- and MrgF-ir nerve fibres (*double arrowheads*) were increased in the lamina propria of the villi (**c**, **d**). *Asterisks* show entrapped parasite eggs. The increased MrgE- and MrgF-ir nerve fibres (*double arrowheads*) in the *S. mansoni*-infected ileum co-expressed calcitonin gene-related peptide (CGRP) to a large extent. In the *inset*, a higher magnification photograph of the MrgE- and MrgF-ir nerve fibres co-expressing CGRP is shown (**e**, **f**). The TNBS-treated ileum showed a reduction in the number of MrgE- and MrgF-ir neuronal perikarya in the enteric plexuses, and immunostained nerve fibres in the tunica muscularis and lamina propria compared to the control ileum (**g**, **h**). *M* mucosa, *CM* circular muscle layer, *LM* longitudinal muscle layer. *Scale bar* 20 µm. *Control* control ileum, *S. mansoni* *S. mansoni*-infected ileum, *TNBS* TNBS-treated ileum

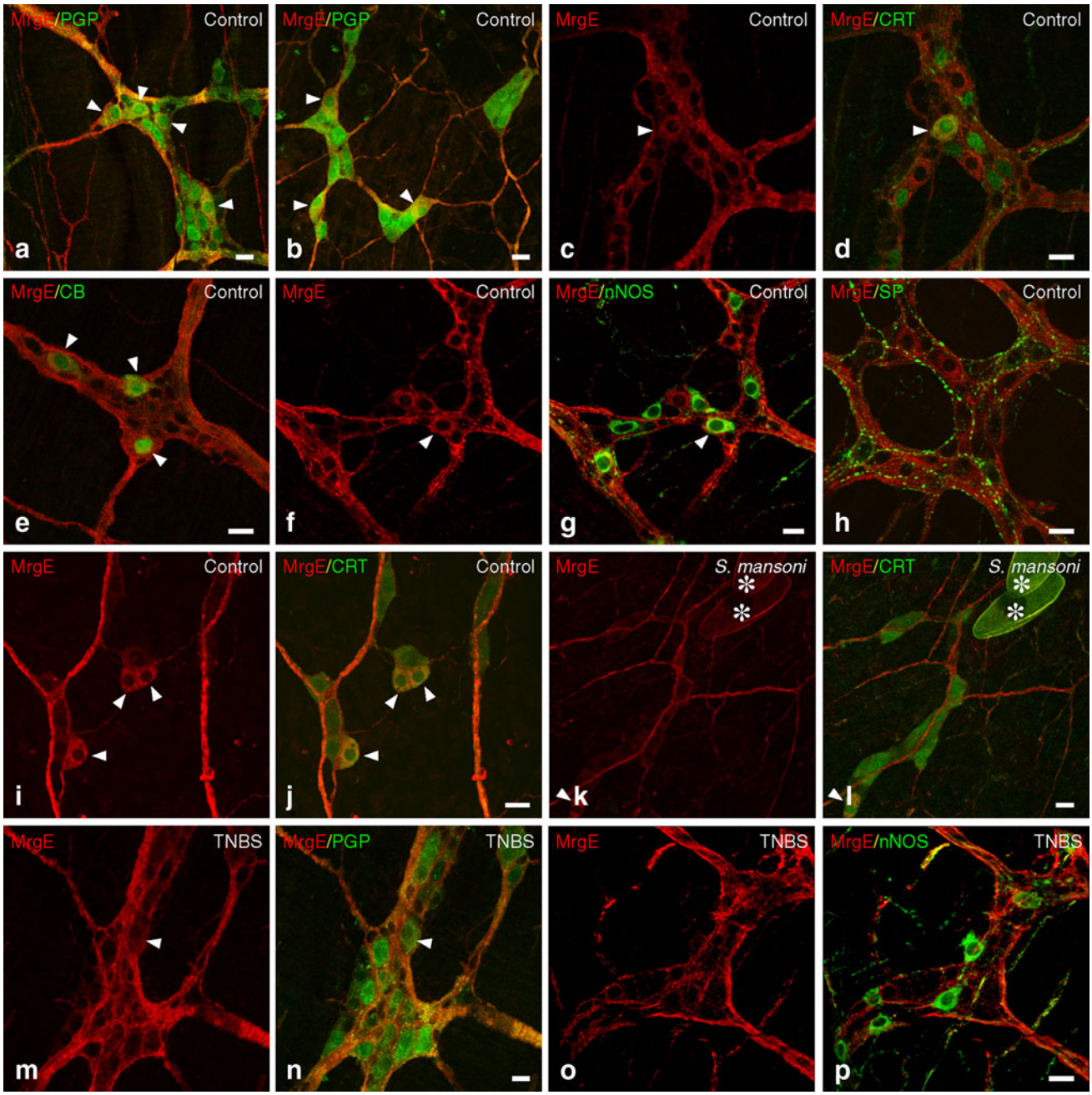

Fig. 4 Expression of MrgE on whole mounts. Co-expression of MrgE and PGP in myenteric (**a**) and submucosal neurons (**b**) in the control ileum. Co-expression of MrgE and CRT (**c**, **d**), MrgE and CB (**e**), MrgE and nNOS (**f**, **g**) and of MrgE and SP (**h**) in myenteric neurons in the control ileum. Co-expression of MrgE and CRT (**i**, **j**) in submucosal neurons in the control ileum. In the *S. mansoni*-infected ileum, the expression of MrgE was significantly reduced in CRT-expressing submucosal neurons in the vicinity of entrapped parasite eggs (*asterisk*) (**k**, **l**). In the TNBS-treated ileum, a significantly decreased proportion of myenteric neurons co-expressing PGP and MrgE (**m**, **n**) was observed; in particular the percentage of MrgE-ir neurons exhibiting nNOS IR was reduced (**o**, **p**). *Arrowheads* double-immunostained neurons. *Scale bar* 20 μm. *Control* control ileum, *S. mansoni S. mansoni*-infected ileum, *TNBS* TNBS-treated ileum

SP (Fig. 5g). Furthermore, 92 ± 3% of the MrgF-ir submucosal neurons displayed CRT IR and 80 ± 3% co-expressed VIP IR (Fig. 5h, i).

In the *S. mansoni*-infected ileum, the proportion of PGP-ir enteric neurons expressing MrgF IR showed a non-significant decrease in the myenteric plexus (8 ± 2%) and was significantly lower in the submucous plexus (5 ± 2%) (Fig. 5j, k). Similar to the MrgE expression, CRT-expressing MrgF-positive submucosal neurons, which were also VIP-negative, were significantly reduced (Table 3).

The TNBS-treated ileum showed a significant reduction in the proportional expression of PGP-ir neurons expressing

Table 3 Quantitative analysis of the immunostainings on whole mounts

Immunoreactive neurons	Co-expressing	Control ileum (%)	*S. mansoni*-infected ileum (%)	TNBS-treated ileum (%)
Myenteric plexus				
PGP	MrgE	17 ± 2	11 ± 3	5 ± 2*
MrgE	CRT	18 ± 2	27 ± 3	30 ± 3
CRT	MrgE	8 ± 2	8 ± 2	5 ± 2
MrgE	CB	50 ± 3	77 ± 3	86 ± 3*
CB	MrgE	26 ± 2	24 ± 2	13 ± 2*
MrgE	nNOS	16 ± 3	13 ± 2	5 ± 2*
nNOS	MrgE	8 ± 2	5 ± 2	<1*
MrgE	SP	6 ± 3	5 ± 2	3 ± 2
SP	MrgE	2 ± 1	1 ± 1	<1
PGP	MrgF	12 ± 2	8 ± 2	4 ± 2*
MrgF	CRT	12 ± 2	16 ± 2	14 ± 2
CRT	MrgF	4 ± 2	4 ± 2	2 ± 1
MrgF	CB	68 ± 3	70 ± 3	90 ± 3*
CB	MrgF	22 ± 2	18 ± 2	13 ± 2*
MrgF	nNOS	15 ± 2	14 ± 2	6 ± 2*
nNOS	MrgF	6 ± 2	4 ± 2	2 ± 1*
MrgF	SP	25 ± 3	30 ± 3	25 ± 3
SP	MrgF	6 ± 2	5 ± 2	3 ± 2
MrgE	MrgF	6 ± 2	nd	nd
MrgF	MrgE	9 ± 2	nd	nd
Submucous plexus				
PGP	MrgE	16 ± 3	8 ± 3*	10 ± 4
MrgE	CRT	80 ± 3	85 ± 2	88 ± 2
CRT	MrgE	15 ± 3	8 ± 3*	10 ± 3
MrgE	VIP	58 ± 3	55 ± 2	85 ± 3
VIP	MrgE	20 ± 3	10 ± 3	18 ± 3
PGP	MrgF	9 ± 2	5 ± 2*	4 ± 2*
MrgF	CRT	92 ± 3	88 ± 3	90 ± 3
CRT	MrgF	10 ± 2	5 ± 2*	4 ± 2*
MrgF	VIP	80 ± 3	85 ± 3	93 ± 3
VIP	MrgF	15 ± 3	9 ± 2	7 ± 3
MrgE	MrgF	32 ± 3	nd	nd
MrgF	MrgE	50 ± 3	nd	nd

Results are expressed as percentages of mean ± standard error of mean

CRT calretinin, *CB* calbindin, *MrgE* Mas-related gene E, *MrgF* Mas-related gene F, *nNOS* neuronal nitric oxide synthase, *PGP* protein gene product 9.5, *SP* substance P, *VIP* vasoactive intestinal peptide, *nd* not done

* $P < 0.05$

MrgF IR (myenteric plexus: 4 ± 2% (Fig. 5l, m); submucous plexus: 4 ± 2%). The proportional distribution of MrgF IR myenteric neurons was only significantly changed for CB (90 ± 3%) and nNOS (6 ± 2%). Also, the percentages of CB-ir and nNOS-ir neurons expressing MrgF IR were significantly decreased (Table 3).

Co-expression of MrgE and MrgF was studied in whole mounts of the control ileum. In the myenteric plexus, only a minor proportion of the MrgE-ir and MrgF-ir neurons displayed the other Mrg receptor (Fig. 6a). In the submucous plexus, half of the MrgF-ir neurons also expressed MrgE IR, while one-third of the MrgE-ir neurons displayed MrgF IR (Fig. 6b–d). It was not possible to perform studies on co-expression of MrgE and MrgF in the two inflammatory models due to technical difficulties dealing with combined immunostainings of MrgE and MrgF in inflammatory conditions.

The results of the quantitative analysis of the neurochemical markers are shown in Table 4. In the control ileum, 54 ± 5% of the PGP-ir myenteric neurons co-expressed CRT (Fig. 7a, b), 29 ± 4% co-expressed CB (Fig. 7c, d), 31 ± 3% yielded nNOS IR (Fig. 7e, f) and 30 ± 3% displayed SP IR (Fig. 7g, h); 93 ± 3% of the PGP-ir submucosal neurons expressed CRT IR (Fig. 7i, j) and 51 ± 3% displayed VIP IR (Fig. 7k, l). Our findings indicate that the proportional expression of neuronal markers used in our study, in the control ileum, is similar to those reported in previous studies (Mongardi Fantaguzzi et al. 2009; Sang

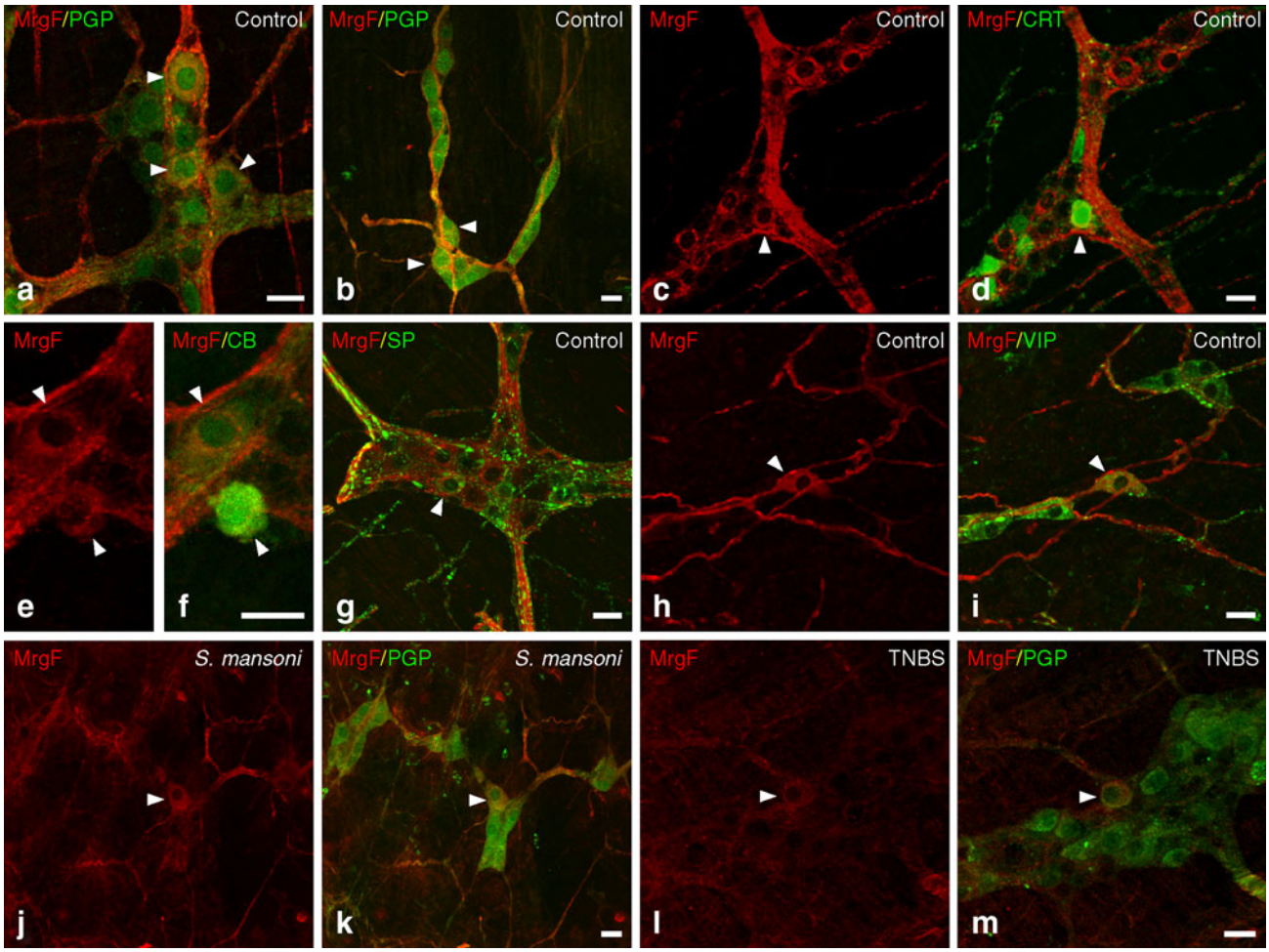

Fig. 5 Expression of MrgF on whole mounts. Co-expression of MrgF and PGP in myenteric (**a**) and submucosal (**b**) neurons in the control ileum. Co-expression of MrgF and CRT (**c**, **d**), MrgF and CB (**e**, **f**) and MrgF and SP (**g**) in myenteric neurons in the control ileum. Co-expression of MrgF and VIP (**h**, **i**) in submucosal neurons in the control ileum. A significantly reduced proportion of PGP-ir submucosal neurons expressed MrgF in the *S. mansoni*-infected ileum (**j**, **k**). A significantly decreased proportion of myenteric neurons co-expressed PGP and MrgF in the TNBS-treated ileum (**l**, **m**). *Arrowheads* double-immunostained neurons. *Scale bar* 20 µm. *Control* control ileum, *S. mansoni* *S. mansoni*-infected ileum, *TNBS* TNBS-treated ileum

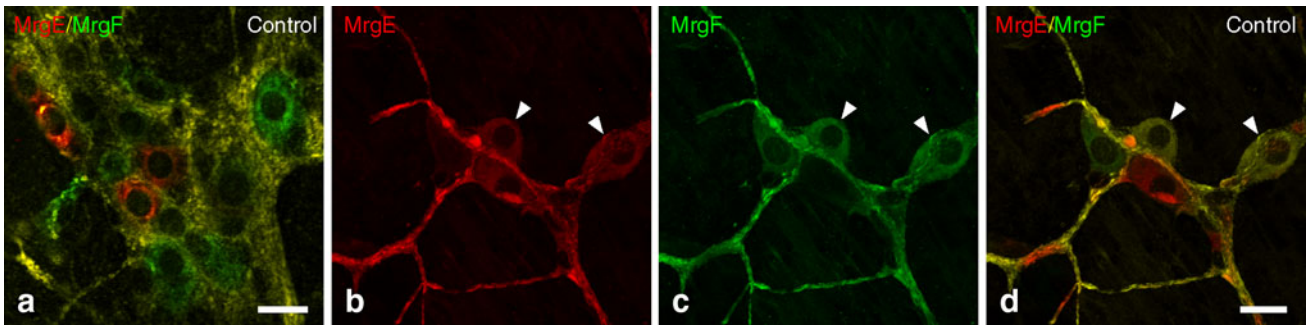

Fig. 6 Co-expression of MrgE and MrgF on whole mounts. Co-expression of MrgE and MrgF in myenteric (**a**) and submucosal (**b**–**d**) neurons in the control ileum. *Arrowheads* double-immunostained neurons. *Scale bar* 20 µm. *Control* control ileum

and Young 1996). The proportional expression of neuronal markers in the *S. mansoni*-infected ileum showed no significant change compared to the control ileum (Table 4). However, in the TNBS-treated ileum, the proportional expression of CB in the myenteric plexus (37 ± 4%) (Table 4; Fig. 7m, n) and of VIP in the submucous plexus (57 ± 4%) (Table 4; Fig. 7o, p) was higher than in the control ileum.

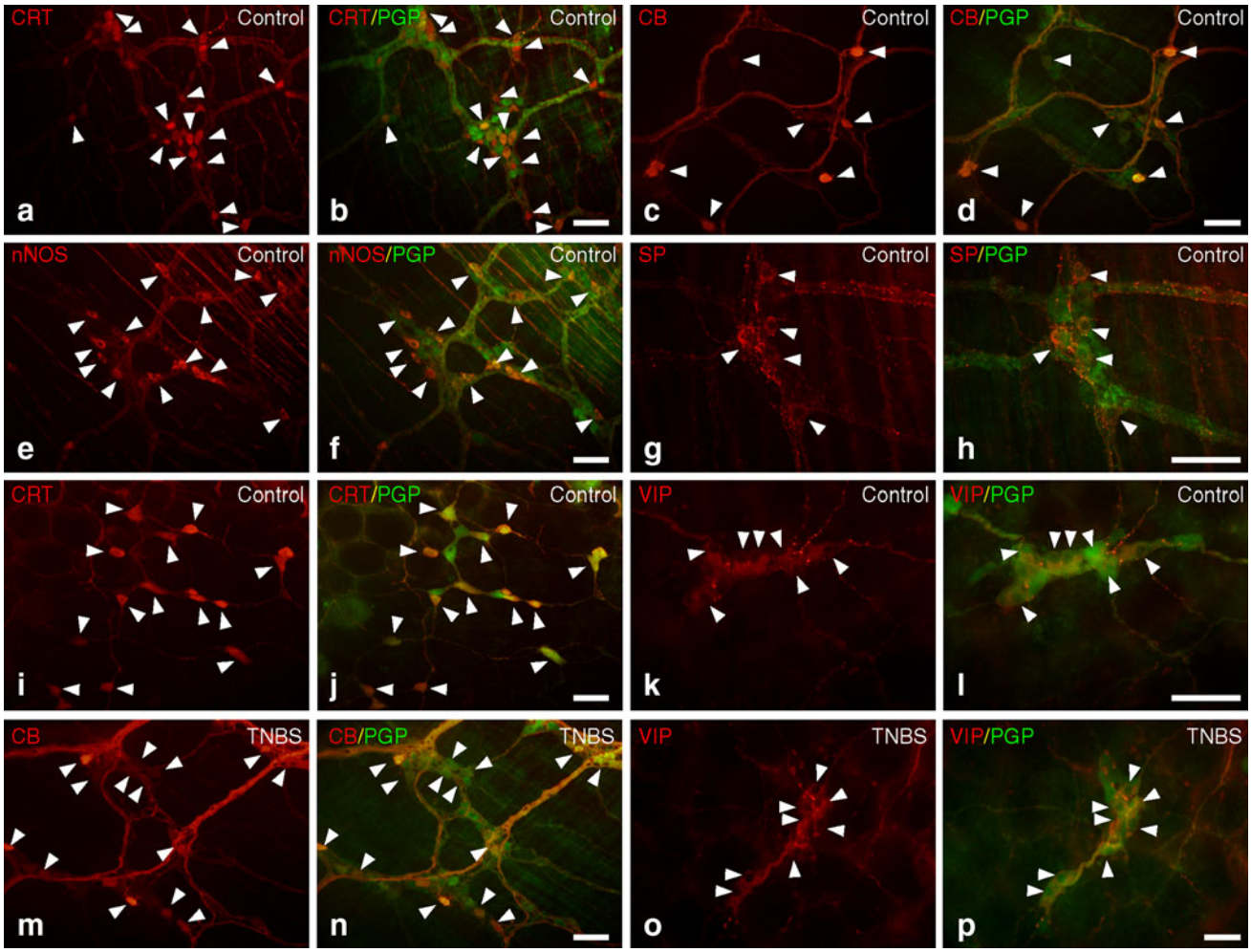

Fig. 7 Expression of neurochemical markers on whole mounts. Co-expression of CRT and PGP (**a**, **b**), CB and PGP (**c**, **d**), nNOS and PGP (**e**, **f**) and SP and PGP (**g**, **h**) in myenteric neurons in the control ileum. Co-expression of CRT and PGP (**i**, **j**) and VIP and PGP (**k**, **l**) in submucosal neurons in the control ileum. In the TNBS-treated ileum, a significantly increased proportion of myenteric neurons co-expressing CB and PGP (**m**, **n**) and submucosal neurons co-expressing VIP and PGP (**o**, **p**) were observed. *Arrowheads* double-immunostained neurons. *Scale bar* 100 µm. *Control* control ileum, *S. mansoni S. mansoni*-infected ileum, *TNBS* TNBS-treated ileum

Table 4 Proportional distribution of neurochemical markers in the enteric plexuses

Immunoreactive neurons	Co-expressing	Control ileum (%)	*S. mansoni*-infected ileum (%)	TNBS-treated ileum (%)
Myenteric plexus				
PGP	CRT	54 ± 5	56 ± 5	54 ± 4
PGP	CB	29 ± 4	33 ± 2	37 ± 4*
PGP	nNOS	31 ± 3	30 ± 3	29 ± 4
PGP	SP	30 ± 3	35 ± 3	33 ± 4
Submucous plexus				
PGP	CRT	93 ± 3	93 ± 3	90 ± 2
PGP	VIP	51 ± 3	53 ± 2	57 ± 4*

Results are expressed as percentages of mean ± standard error of mean

CRT calretinin, *CB* calbindin, *nNOS* neuronal nitric oxide synthase, *PGP* protein gene product 9.5, *SP* substance P, *VIP* vasoactive intestinal peptide

* $P < 0.05$

Discussion

This study presents the first data in mouse on the expression of the MrgE and MrgF receptors in distinct subpopulations of enteric neurons and nerve fibres, in both physiological and pathophysiological conditions, i.e. in healthy controls, and in two distinct intestinal inflammation models, namely, intestinal schistosomiasis and TNBS-induced ileitis.

It has previously been suggested that MrgE is expressed at all tissue levels involved in pain sensation and that MrgE influences the expression level of MrgF (Cox et al. 2008). The GI tract is richly endowed with sensory elements, such as the enteric neurons that monitor the gut environment and activate local or central reflex circuits. Abdominal or visceral pain can be a manifestation of impending injury or harm to the gut and may arise from several mechanisms including intestinal inflammation. The spinal and vagal nerve pathways play an important role in such abdominal pain sensations, but the role of enteric neurons cannot be neglected (Bielefeldt et al. 2009; Blackshaw et al. 2007). Therefore, it is expected that Mrg receptors, such as MrgE and MrgF, are expressed in some enteric neurons. A previous attempt to detect MrgE mRNA in the small and large intestine failed (Zhang et al. 2005), whereas MrgF mRNA had previously been demonstrated in the rat stomach and intestine (Ross et al. 1990). In rat, MrgA mRNA and MrgC mRNA were observed in the wall of the GI tract, but no information on cellular expression was provided in this study (Gustafson et al. 2005). Furthermore, the only other Mrg receptor detected in the GI tract, more precisely in the ENS, is MrgX2 in man (Allia et al. 2005; Robas et al. 2003). Gastrointestinal inflammation is known to be associated with enteric neuroplasticity and changes in neurochemistry, the mechanisms of which may differ amongst the inflammatory models that have been used. In other words, it has been shown that responses of the ENS to inflammation may vary according to the site and type of inflammation based on the inflammatory stimulus (Giaroni et al. 1999; Lomax et al. 2005; Mawe et al. 2009; Vasina et al. 2006). Therefore, in our study dealing with the effect of inflammation on the expression of MrgE and MrgF, two distinct models of intestinal inflammation were used, to allow for the identification of possible model specific effects. We report in detail the expression and distribution of MrgE and MrgF in enteric neurons in the non-inflamed control, as well as in the two distinct intestinal inflammatory conditions.

The present study clearly revealed that MrgE and MrgF receptors are expressed in distinct neuronal types in both enteric plexuses. In the myenteric plexus, we observed a neuronal subpopulation expressing MrgE, another subpopulation expressing MrgF and a small subpopulation (<1% of the myenteric neurons) bearing both Mrg receptors. The major part of MrgE-ir and MrgF-ir neurons displayed CB, predominantly expressed in mouse in intrinsic primary afferent or sensory neurons (IPANs) (Qu et al. 2008). Co-expression with CRT and nNOS was also observed in some MrgE-ir and MrgF-ir neurons. In mouse, CRT is expressed in one-third of the sensory neurons, in excitatory motor neurons and in some interneurons, while nNOS is found in inhibitory motor neurons and in some interneurons (Qu et al. 2008). A small proportion of MrgE-ir and MrgF-ir neurons also contained SP, which in mouse is present in the excitatory motor neurons and ascending interneurons (Qu et al. 2008). These observations lead us to assume that MrgE and MrgF are not only found in myenteric sensory neurons, but also in some motor neurons and interneurons.

In the submucous plexus, we observed three neuronal subpopulations of equal proportion expressing MrgE, MrgF or both Mrg receptors. Almost all MrgF-ir neurons displayed VIP and CRT IR, while only half of the MrgE-ir neurons expressed VIP IR, in contrast to CRT, which was found in almost all MrgE-ir neurons. It has previously been reported that more than 90% of all submucosal neurons contain CRT, while approximately half of the submucosal neurons, being secretomotor or vasodilator neurons, express VIP IR (Mongardi Fantaguzzi et al. 2009). This indicates that the majority of the MrgE-ir and MrgF-ir submucosal neurons are secretomotor or vasodilator neurons.

Inflammation was found to reduce the expression and presence of MrgE and MrgF in enteric neuronal somata, as demonstrated by both inflammation models, and this decrease was more pronounced in the TNBS-treated condition. In the *S. mansoni*-infected ileum, there were no significant changes in MrgE or MrgF expression in the myenteric plexus, in contrast to the submucous plexus where less VIP-negative neurons expressed MrgE or MrgF. Since there were no significant changes in the proportional expression of neuronal markers in the *S. mansoni*-infected ileum, this decreased MrgE or MrgF subpopulation is solely assumed to contain cholinergic secretomotor neurons, according to the previous neurochemical coding study of Mongardi Fantaguzzi et al. (2009). This decrease in MrgE and MrgF IR, especially in the vicinity of entrapped parasite eggs, may be related to the effect of the granulomatous inflammation around the eggs. The trend towards downregulation of MrgE and MrgF mRNA levels in the *S. mansoni*-infected ileum could therefore be attributed to the decreased MrgE and MrgF expression in submucosal neurons. Although the number of neuronal somata expressing MrgE or MrgF receptors was reduced in enteric neurons during intestinal schistosomiasis, we observed an increase in the number of nerve fibres expressing MrgE or MrgF in the lamina propria of the villi. Previous studies have shown that CGRP-expressing extrinsic sensory neurons project to the ileum and that the density and number of extrinsically

derived CGRP-ir nerve fibres in the lamina propria of the villi are conspicuously increased during the acute phase of intestinal schistosomiasis in mouse (De Jonge et al. 2003; Van Op den bosch et al. 2007). Linking this information to our findings of the extensive co-expression of MrgE and MrgF IR nerve fibres with CGRP and recalling that MrgE and MrgF are expressed in spinal sensory neurons in mouse (Cox et al. 2008; Zhang et al. 2005), it can be suggested that the major part of the MrgE- or MrgF-expressing nerve fibres are extrinsic in origin during intestinal schistosomiasis. Taken together, the mechanisms of neuroplasticity of MrgE and MrgF-expressing neurons in this parasitic model possibly seem to differ between intrinsic versus extrinsic neurons.

During TNBS-induced inflammation, in the myenteric plexus, less PGP-ir myenteric neurons, especially less nitrergic neurons, expressed MrgE or MrgF. The increased co-expression of MrgE and MrgF with CB in this condition may be interpreted as a consequence of the increased proportional expression of CB in the myenteric plexus during TNBS-induced inflammation, as observed from the findings of the qualitative analysis of neurochemical markers. Further, while no significant changes were observed for MrgE in the submucous plexus in the TNBS-treated ileum, less VIP-negative neurons stained for MrgF. Acute TNBS-induced inflammation is a model of acute mucosal damage and a localized Th1/Th17-type inflammatory reaction, which is self-limiting, with eventual production of regulatory cytokines shortly after the acute stage (Pontell et al. 2009; Ruyssers et al. 2009). Therefore, the decreased proportions of MrgE or MrgF-expressing myenteric neurons, in particular the nitrergic neurons in the TNBS-induced ileitis model, are probably related to the severe and local histological changes occurring during this type of inflammation, which might have affected the motoric or interneuronal expression of MrgE or MrgF. Although the qualitative analysis of neurochemical markers demonstrated increased proportional expression of VIP in submucosal neurons in this condition, there seem to be no significant changes with respect to the MrgE or MrgF expression in VIP neurons. The decreased proportion of MrgF-expressing submucosal neurons in this condition may be MrgF-expressing cholinergic secretomotor neurons. Furthermore, in this condition, we did not observe any nerve fibre sprouting in the lamina propria of the villi, which is most likely due to the histological ablation of the villi in this condition. The significant downregulation of MrgE mRNA level in the TNBS-treated ileum could be attributed to the decreased expression of MrgE in myenteric neurons, and that for the MrgF mRNA level to the decreased expression of MrgF in myenteric as well as submucosal neurons. The present results, however, did not reveal if the observed reduction was due to neuronal loss. Previously, it has been reported in mouse that neuronal cell death is rarely observed during intestinal schistosomiasis (Bogers et al. 2000; Van Nassauw et al. 2001). A significant loss of myenteric neurons was observed in the TNBS-inflamed guinea pig colon, as early as 12 h after TNBS administration (Linden et al. 2005), while in another study on guinea pigs, TNBS-induced ileitis was shown to cause phenotypic changes in the myenteric neurons (Nurgali et al. 2007).

A study on mouse involving deletion of *MrgE* reported that this deletion increased the MrgF gene expression in the spinal cord, suggesting that MrgE expression regulates MrgF expression at some tissue levels (Cox et al. 2008). In the present study, no increased expression of MrgF was observed, although MrgE expression in enteric neuronal cell bodies diminished during inflammation. This may be due to the observation that only a minor proportion of enteric neurons co-expressed both Mrg receptors, which is in contrast to the spinal cord, where it has been assumed that both Mrg receptors are co-expressed (Cox et al. 2008).

It is generally assumed that Mrg receptors are expressed mainly in sensory neurons and implicated in nociception. In concordance with the above, the present study demonstrates the expression of MrgE and MrgF in enteric sensory neurons. In addition to this, our results show that expression of MrgE and MrgF is not limited to IPANs. A recent study revealed that mechanosensitivity is a property of more enteric neuronal subpopulations than generally assumed and that every subpopulation of enteric neurons is to some extent sensitive to mechanical distortion, which might imply that the current concept of sensory transmission in the ENS needs to be revised (Mazzuoli and Schemann 2009). In previous studies in rat, MrgA, MrgC and MrgF mRNAs were detected in the cerebellum, i.e. the centre of motor coordination (Gustafson et al. 2005; Ross et al. 1990); more interestingly, in the human cerebellum, MrgE mRNA was found in Golgi cells, which are considered inhibitory interneurons, and in Purkinje cells, which perform inhibitory motor functions (Zhang et al. 2005). Recent studies in the cerebellar biology indicate that there may be a role for this organ in nociception and mechanosensation (Duggan et al. 2002; Edvinsson et al. 2011). Taken together, all these data demonstrate that Mrg receptors are not exclusively expressed in sensory neurons, but also in some non-sensory neurons which may be involved in mechanosensation and nociception.

To conclude, the present results demonstrate in the murine ileum the expression and distribution of the Mrg receptors, MrgE and MrgF in enteric neurons. Both MrgE and MrgF receptors were present in distinct neuronal types, such as sensory neurons, some motor neurons, interneurons and secretomotor or vasodilator neurons. Only a minor proportion of enteric neurons co-expressed MrgE and MrgF.

The expression and presence of both MrgE and MrgF receptors in enteric neurons were negatively affected by intestinal inflammation. In intestinal schistosomiasis, a lower number of cholinergic secretomotor submucosal neurons, especially in the vicinity of entrapped parasite eggs, expressed MrgE or MrgF. Furthermore, there is an indication of extrinsic afferent contribution of MrgE and MrgF in this condition. In TNBS-ileitis, a lower number of nitrergic motor or interneurons in the myenteric plexus expressed MrgE or MrgF, and a lower number of cholinergic secretomotor submucosal neurons expressed MrgF. The downregulation of MrgE in enteric neurons did not result in a compensatory effect by MrgF in either of the intestinal inflammatory models. The findings in this study indicate plasticity of MrgE and MrgF-expressing neurons during intestinal inflammation. Although ligands are identified for some members of the Mrg family, the lack of knowledge of specific (ant)agonists acting on MrgE or MrgF hinders the possibility of further functional elucidation of MrgE and MrgF. Further studies aiming at identifying specific (ant)agonists acting on MrgE and MrgF will help unravel the physiological role of these Mrg receptors in intestinal inflammation. Given the presence of clear orthologues for *MrgE* and *MrgF* in humans that bear some similarities to their murine counterparts, these data from murine models should provide valuable information about MrgE and MrgF receptors both in mice and humans.

Acknowledgments The authors thank the staff of the Laboratory of Cell biology and Histology for their excellent technical assistance. This study was funded by a grant of the Flemish Organization for Scientific Research (FWO G.0179.08) and by a TOP-BOF (2008–2011) project of the University of Antwerp.

References

Allia E, Tarabra E, Volante M, Cerrato M, Ghigo E, Muccioli G, Papotti M (2005) Expression of cortistatin and MrgX2, a specific cortistatin receptor, in human neuroendocrine tissues and related tumours. J Pathol 207:336–345

Bender E, Buist A, Jurzak M, Langlois X, Baggerman G, Verhasselt P, Ercken M, Guo HQ, Wintmolders C, Van dW I, Van Oers I, Schoofs L, Luyten W (2002) Characterization of an orphan G protein-coupled receptor localized in the dorsal root ganglia reveals adenine as a signaling molecule. Proc Natl Acad Sci USA 99:8573–8578

Bielefeldt K, Davis B, Binion DG (2009) Pain and inflammatory bowel disease. Inflamm Bowel Dis 15:778–788

Blackshaw LA, Brookes SJ, Grundy D, Schemann M (2007) Sensory transmission in the gastrointestinal tract. Neurogastroenterol Motil 19:1–19

Bogers J, Moreels T, De Man J, Vrolix G, Jacobs W, Pelckmans P, Van Marck E (2000) *Schistosoma mansoni* infection causing diffuse enteric inflammation and damage of the enteric nervous system in the mouse small intestine. Neurogastroenterol Motil 12:431–440

Breit A, Gagnidze K, Devi LA, Lagace M, Bouvier M (2006) Simultaneous activation of the delta opioid receptor (deltaOR)/sensory neuron-specific receptor-4 (SNSR-4) hetero-oligomer by the mixed bivalent agonist bovine adrenal medulla peptide 22 activates SNSR-4 but inhibits deltaOR signaling. Mol Pharmacol 70:686–696

Burstein ES, Ott TR, Feddock M, Ma JN, Fuhs S, Wong S, Schiffer HH, Brann MR, Nash NR (2006) Characterization of the Mas-related gene family: structural and functional conservation of human and rhesus MrgX receptors. Br J Pharmacol 147:73–82

Chang M, Li W, Peng YL, Gao YH, Yao J, Han RW, Wang R (2009) Involvement of NMDA receptor in nociceptive effects elicited by intrathecal [Tyr6] gamma2-MSH(6–12), and the interaction with nociceptin/orphanin FQ in pain modulation in mice. Brain Res 1271:36–48

Chen H, Ikeda SR (2004) Modulation of ion channels and synaptic transmission by a human sensory neuron-specific G-protein-coupled receptor, SNSR4/mrgX1, heterologously expressed in cultured rat neurons. J Neurosci 24:5044–5053

Cox PJ, Pitcher T, Trim SA, Bell CH, Qin W, Kinloch RA (2008) The effect of deletion of the orphan G protein-coupled receptor (GPCR) gene MrgE on pain-like behaviours in mice. Mol Pain 4:2

Crozier RA, Ajit SK, Kaftan EJ, Pausch MH (2007) MrgD activation inhibits KCNQ/M-currents and contributes to enhanced neuronal excitability. J Neurosci 27:4492–4496

De Jonge F, Van Nassauw L, Van Meir F, Miller HR, Van Marck E, Timmermans JP (2002) Temporal distribution of distinct mast cell phenotypes during intestinal schistosomiasis in mice. Parasite Immunol 24:225–231

De Jonge F, Van Nassauw L, Adriaensen D, Van Meir F, Miller HR, Van Marck E, Timmermans JP (2003) Effect of intestinal inflammation on capsaicin-sensitive afferents in the ileum of *Schistosoma mansoni*-infected mice. Histochem Cell Biol 119:477–484

Dong X, Han S, Zylka MJ, Simon MI, Anderson DJ (2001) A diverse family of GPCRs expressed in specific subsets of nociceptive sensory neurons. Cell 106:619–632

Duggan A, Garcia-Anoveros J, Corey DP (2002) The PDZ domain protein PICK1 and the sodium channel BNaC1 interact and localize at mechanosensory terminals of dorsal root ganglion neurons and dendrites of central neurons. J Biol Chem 277:5203–5208

Dussor G, Zylka MJ, Anderson DJ, McCleskey EW (2008) Cutaneous sensory neurons expressing the Mrgprd receptor sense extracellular ATP and are putative nociceptors. J Neurophysiol 99:1581–1589

Edvinsson L, Eftekhari S, Salvatore CA, Warfvinge K (2011) Cerebellar distribution of calcitonin gene-related peptide (CGRP) and its receptor components calcitonin receptor-like receptor (CLR) and receptor activity modifying protein 1 (RAMP1) in rat. Mol Cell Neurosci 46:333–339

Elson CO, Beagley KW, Sharmanov AT, Fujihashi K, Kiyono H, Tennyson GS, Cong Y, Black CA, Ridwan BW, McGhee JR (1996) Hapten-induced model of murine inflammatory bowel disease: mucosa immune responses and protection by tolerance. J Immunol 157:2174–2185

Gembardt F, Grajewski S, Vahl M, Schultheiss HP, Walther T (2008) Angiotensin metabolites can stimulate receptors of the Mas-related genes family. Mol Cell Biochem 319:115–123

Giaroni C, De Ponti F, Cosentino M, Lecchini S, Frigo G (1999) Plasticity in the enteric nervous system. Gastroenterology 117:1438–1458

Grazzini E, Puma C, Roy MO, Yu XH, O'Donnell D, Schmidt R, Dautrey S, Ducharme J, Perkins M, Panetta R, Laird JM, Ahmad S, Lembo PM (2004) Sensory neuron-specific receptor activation elicits central and peripheral nociceptive effects in rats. Proc Natl Acad Sci USA 101:7175–7180

Gustafson EL, Maguire M, Campanella M, Tarozzo G, Jia Y, Dong XW, Laverty M, Murgolo N, Priestley T, Reggiani A, Monsma F, Beltramo M (2005) Regulation of two rat mas-related genes in a model of neuropathic pain. Brain Res Mol Brain Res 142:58–64

Hager UA, Hein A, Lennerz JK, Zimmermann K, Neuhuber WL, Reeh PW (2008) Morphological characterization of rat Mas-related G-protein-coupled receptor C and functional analysis of agonists. Neuroscience 151:242–254

Han SK, Dong X, Hwang JI, Zylka MJ, Anderson DJ, Simon MI (2002) Orphan G protein-coupled receptors MrgA1 and MrgC11 are distinctively activated by RF-amide-related peptides through the Galpha q/11 pathway. Proc Natl Acad Sci USA 99:14740–14745

Kamohara M, Matsuo A, Takasaki J, Kohda M, Matsumoto M, Matsumoto S, Soga T, Hiyama H, Kobori M, Katou M (2005) Identification of MrgX2 as a human G-protein-coupled receptor for proadrenomedullin N-terminal peptides. Biochem Biophys Res Commun 330:1146–1152

Kunapuli P, Lee S, Zheng W, Alberts M, Kornienko O, Mull R, Kreamer A, Hwang JI, Simon MI, Strulovici B (2006) Identification of small molecule antagonists of the human mas-related gene-X1 receptor. Anal Biochem 351:50–61

Lee MG, Dong X, Liu Q, Patel KN, Choi OH, Vonakis B, Undem BJ (2008) Agonists of the MAS-related gene (Mrgs) orphan receptors as novel mediators of mast cell–sensory nerve interactions. J Immunol 180:2251–2255

Lembo PM, Grazzini E, Groblewski T, O'Donnell D, Roy MO, Zhang J, Hoffert C, Cao J, Schmidt R, Pelletier M, Labarre M, Gosselin M, Fortin Y, Banville D, Shen SH, Strom P, Payza K, Dray A, Walker P, Ahmad S (2002) Proenkephalin A gene products activate a new family of sensory neuron-specific GPCRs. Nat Neurosci 5:201–209

Lewis Carl SA, Gillete-Ferguson I, Ferguson DG (1993) An indirect immunofluorescence procedure for staining the same cryosection with two mouse monoclonal primary antibodies. J Histochem Cytochem 41:1273–1278

Linden DR, Couvrette JM, Ciolino A, McQuoid C, Blaszyk H, Sharkey KA, Mawe GM (2005) Indiscriminate loss of myenteric neurones in the TNBS-inflamed guinea-pig distal colon. Neurogastroenterol Motil 17:751–760

Liu Y, Yang FC, Okuda T, Dong X, Zylka MJ, Chen CL, Anderson DJ, Kuner R, Ma Q (2008) Mechanisms of compartmentalized expression of Mrg class G-protein-coupled sensory receptors. J Neurosci 28:125–132

Llewellyn-Smith IJ, Costa M, Furness JB (1985) Light and electron microscopic immunocytochemistry of the same nerves from whole-mount preparations. J Histochem Cytochem 33:857–866

Lomax AE, Fernandez E, Sharkey KA (2005) Plasticity of the enteric nervous system during intestinal inflammation. Neurogastroenterol Motil 17:4–15

Mawe GM, Strong DS, Sharkey KA (2009) Plasticity of enteric nerve functions in the inflamed and postinflamed gut. Neurogastroenterol Motil 21:481–491

Mazzuoli G, Schemann M (2009) Multifunctional rapidly adapting mechanosensitive enteric neurons (RAMEN) in the myenteric plexus of the guinea pig ileum. J Physiol 587:4681–4694

Milasta S, Pediani J, Appelbe S, Trim S, Wyatt M, Cox P, Fidock M, Milligan G (2006) Interactions between the Mas-related receptors MrgD and MrgE alter signalling and trafficking of MrgD. Mol Pharmacol 69:479–491

Mongardi Fantaguzzi C, Thacker M, Chiocchetti R, Furness JB (2009) Identification of neuron types in the submucosal ganglia of the mouse ileum. Cell Tissue Res 336:179–189

Negoescu A, Labat-Moleur F, Lorimier P, Lamarcq L, Guillermet C, Chambaz E, Brambilla E (1994) F(ab) secondary antibodies: a general method for double immunolabelling with primary antisera from the same species. Efficiency control by chemiluminescence. J Histochem Cytochem 42:433–437

Nurgali K, Nguyen TV, Matsuyama H, Thacker M, Robbins HL, Furness JB (2007) Phenotypic changes of morphologically identified guinea-pig myenteric neurons following intestinal inflammation. J Physiol 583:593–609

Pontell L, Castelucci P, Bagyanszki M, Jovic T, Thacker M, Nurgali K, Bron R, Furness JB (2009) Structural changes in the epithelium of the small intestine and immune cell infiltration of enteric ganglia following acute mucosal damage and local inflammation. Virchows Arch 455:55–65

Qu ZD, Thacker M, Castelucci P, Bagyanszki M, Epstein ML, Furness JB (2008) Immunohistochemical analysis of neuron types in the mouse small intestine. Cell Tissue Res 334:147–161

Rau KK, McIlwrath SL, Wang H, Lawson JJ, Jankowski MP, Zylka MJ, Anderson DJ, Koerber HR (2009) Mrgprd enhances excitability in specific populations of cutaneous murine polymodal nociceptors. J Neurosci 29:8612–8619

Robas N, Mead E, Fidock M (2003) MrgX2 is a high potency cortistatin receptor expressed in dorsal root ganglion. J Biol Chem 278:44400–44404

Ross PC, Figler RA, Corjay MH, Barber CM, Adam N, Harcus DR, Lynch KR (1990) RTA, a candidate G protein-coupled receptor: cloning, sequencing, and tissue distribution. Proc Natl Acad Sci USA 87:3052–3056

Ruyssers NE, De Winter BY, De Man JG, Loukas A, Pearson MS, Weinstock JV, Van den Bossche RM, Martinet W, Pelckmans PA, Moreels TG (2009) Therapeutic potential of helminth soluble proteins in TNBS-induced colitis in mice. Inflamm Bowel Dis 15:491–500

Sang Q, Young HM (1996) Chemical coding of neurons in the myenteric plexus and external muscle of the small and large intestine of the mouse. Cell Tissue Res 284:39–53

Shinohara T, Harada M, Ogi K, Maruyama M, Fujii R, Tanaka H, Fukusumi S, Komatsu H, Hosoya M, Noguchi Y, Watanabe T, Moriya T, Itoh Y, Hinuma S (2004) Identification of a G protein-coupled receptor specifically responsive to beta-alanine. J Biol Chem 279:23559–23564

Tatemoto K, Nozaki Y, Tsuda R, Konno S, Tomura K, Furuno M, Ogasawara H, Edamura K, Takagi H, Iwamura H, Noguchi M, Naito T (2006) Immunoglobulin E-independent activation of mast cell is mediated by Mrg receptors. Biochem Biophys Res Commun 349:1322–1328

Van Nassauw L, Bogers J, Van Marck E, Timmermans JP (2001) Role of reactive nitrogen species in neuronal cell damage during intestinal schistosomiasis. Cell Tissue Res 303:329–336

Van Nassauw L, Brouns I, Adriaensen D, Burnstock G, Timmermans JP (2002) Neurochemical identification of enteric neurons expressing $P2X_3$ receptors in the guinea-pig ileum. Histochem Cell Biol 118:193–203

Van Op den bosch J, Van Nassauw L, Lantermann K, Van Marck E, Timmermans JP (2007) Effect of intestinal inflammation on the cell-specific expression of somatostatin receptor subtypes in the murine ileum. Neurogastroenterol Motil 19:596–606

Vasina V, Barbara G, Talamonti L, Stanghellini V, Corinaldesi R, Tonini M, De Ponti F, De Giorgio R (2006) Enteric neuroplasticity evoked by inflammation. Auton Neurosci 126–127:264–272

Vella AT, Pearce EJ (1992) CD4+ Th2 response induced by *Schistosoma mansoni* eggs develops rapidly, through an early, transient, Th0-like stage. J Immunol 148:2283–2290

Wang H, Zylka MJ (2009) Mrgprd-expressing polymodal nociceptive neurons innervate most known classes of substantia gelatinosa neurons. J Neurosci 29:13202–13209

Wang Z, Takahashi T, Saito Y, Nagasaki H, Ly NK, Nothacker HP, Reinscheid RK, Yang J, Chang JK, Shichiri M, Civelli O (2006) Salusin beta is a surrogate ligand of the mas-like G protein-coupled receptor MrgA1. Eur J Pharmacol 539:145–150

Wroblowski B, Wigglesworth MJ, Szekeres PG, Smith GD, Rahman SS, Nicholson NH, Muir AI, Hall A, Heer JP, Garland SL, Coates

WJ (2009) The discovery of a selective, small molecule agonist for the MAS-related gene X1 receptor. J Med Chem 52:818–825

Yolles TK, Moore DV, Meleney HE (1949) Post-cercarial development of *Schistosoma mansoni* in the rabbit and hamster after intraperitoneal and percutaneous infection. J Parasitol 35:276–294

Young D, Waitches G, Birchmeier C, Fasano O, Wigler M (1986) Isolation and characterization of a new cellular oncogene encoding a protein with multiple potential transmembrane domains. Cell 45:711–719

Zhang L, Taylor N, Xie Y, Ford R, Johnson J, Paulsen JE, Bates B (2005) Cloning and expression of MRG receptors in macaque, mouse, and human. Brain Res Mol Brain Res 133:187–197

Zylka MJ, Dong X, Southwell AL, Anderson DJ (2003) Atypical expansion in mice of the sensory neuron-specific Mrg G protein-coupled receptor family. Proc Natl Acad Sci USA 100:10043–10048